EASR

Engineering and Applied Science Research

https://www.tci-thaijo.org/index.php/easr/index

Published by the Faculty of Engineering, Khon Kaen University, Thailand

Effect of an in vitro environment on compressive strength and apatite formation of white Portland cement

Weerapol Taptimdee[1)], Auttachai Jantasang[1)], Prinya Chindaprasirt[2, 3)], Yuichi Otsuka[4)], Yoshiharu Mutoh[5)], and Teerawat Laonapakul*[1)]

[1)]Department of Industrial Engineering, Faculty of Engineering, Khon Kaen University, Khon Kaen 40002, Thailand
[2)]Sustainable Infrastructure Research and Development Center, Department of Civil Engineering, Faculty of Engineering, Khon Kaen University, Khon Kaen 40002, Thailand
[3)]Academy of Science, The Royal Society of Thailand, Bangkok 10300, Thailand
[4)]Department of System Safety, Nagaoka University of Technology, Nagaoka, Niigata 940-2188, Japan
[5)]Nagaoka University of Technology, Nagaoka, Niigata 940-2188, Japan

Received 30 January 2021
Revised 19 May 2021
Accepted 28 May 2021

Abstract

The density, porosity and compressive strength of white Portland cement (WPC) samples were evaluated to study their potential for use for bone implant applications. The effects of simulated body fluid (SBF) solution on the compressive strengths of WPC samples were also examined by immersing the sample in an SBF solution. The formation of bone-like apatite on the surface and in the internal structure of the WPC samples after immersion in an SBF solution was investigated. After 28 days of water curing, the compressive strength and porosity of the WPC samples were 51.88 MPa and 41.83%, respectively. The WPC samples tested after immersion in an SBF solution showed an improvement in compressive strength at approximately 13 percent, which is a good indicator for its use as a bone implant material. Bone-like apatite was apparently formed on the surfaces and in the internal structures of WPC samples after 28 days of immersion in an SBF solution. The thickness of the bone-like apatite forming was about 30 μm.

Keywords: In vitro test, Simulated body fluid, Apatite formation, Physical and mechanical property

1. Introduction

A number of bone substitutes and bone graft materials have been developed as alternatives for bone repair, augmentation or substitution. The primary target of bone substitute material research is to develop materials that have physical, chemical and mechanical properties similar to human bone. The mechanical property of the bone substitute materials should be in close association with the mechanical property of the surrounding bone. The bone substitute materials should retain its mechanical property after implantation to reconstruct hard load-bearing tissues. The variation in mechanical property due to the degradation process should be compatible with the bone regeneration process [1]. Among the mechanical properties evaluated, compressive strength is usually employed to characterize the mechanical behavior of bone substitutes [2]. Additionally, the formation of bone-like apatite on the surface of an artificial bone implant material is a necessary requirement after implantation into a living body [3, 4]. The bone-bonding ability of bone substitute materials is usually determined by evaluating their ability to form bone-like apatite on the surface using *in vitro* testing in a simulated body fluid (SBF) solution with an ionic concentration mimicking that of human blood plasma. This method has been widely applied for *in vitro* evaluation of bioactivity and assessment of bone-like apatite formation on various artificial bone implant materials [5-8]. This implies that the *in vivo* bone bioactivity of the implant materials can be anticipated from the formation of bone-like apatite observed on their surfaces during *in vitro* testing in an SBF solution.

Hydroxyapatite (HAp) is an ideal material for artificial bones because it has excellent biocompatibility, bioactivity and osteoconductivity. It is also used as a coating on metallic biomaterials to improve the bioactive properties of the surfaces of implants. Out of the various available coating techniques, plasma spraying is one of the more commercially accepted methods used to apply hydroxyapatite coatings for biomedical applications. The extremely high temperature of the plasma spray, however, can cause decomposition of the coating, instability of the coating-substrate interface and an unstable coating duration in body fluids and under local variable loading [9, 10]. Moreover, the decreasing quality of the mechanical properties of HAp coatings on metal substrates during immersion in physiological solutions remains a problem [11-14].

White Portland cement (WPC), which mainly consists of tricalcium silicate (Ca_3SiO_5) and dicalcium silicate (Ca_2SiO_4), is a common construction material with a strength development at ambient temperatures similar to ordinary Portland cement. The composition, room-temperature solidification and white colour with non-toxicity of this calcium silicate material give it biomedical potential for use as a bone substitute or coating material for biomedical applications. A number of research studies on calcium silicate-based materials have investigated their potential medical use in bone and dental applications [15-20]. Coleman et al. [21, 22], Torkittikul

*Corresponding author. Tel.: +668 5916 0505
Email address: teerla@kku.ac.th
doi: 10.14456/easr.2022.20

and Chaipanich [23] performed a preliminary evaluation of the *in vitro* biological properties of WPC. They demonstrated that a bone-like apatite layer is precipitated on the surface of WPC within a week of immersion in an SBF solution. They also clarified that the silicate group in WPC is an important substrate which nucleates bone-like apatite on WPC surfaces. The bone-like apatite precipitation on the WPC surface is caused by the dissolution of calcium hydroxide ($Ca(OH)_2$) from WPC into an SBF solution. The increasing of Ca^+ ions enhance the supersaturation of SBF solution, which promotes the deposition of bone-like apatite on the WPC surface [21-23]. A rapidly hardening Portland cement utilizing calcium chloride has also been developed and evaluated for use as a restorative material and its toxicity to SaOS-2 cells was evaluated [24]. The mechanical property of WPC was studied by Torkittikul and Chaipanich [23]. The high compressive strength was achieved after curing WPC in water for 7 days. In the literature, the strength of WPC was studied only after curing in water. There has been no study aim at examining of mechanical property of WPC after apatite precipitation on its surface by the *in vitro* biological test. Some important considerations, including the effects of the *in vitro* environment on the mechanical and physical properties of WPC, have not been fully reported and require investigation before the study of WPC coating on metallic implants and other applications.

In this study, *in vitro* biological tests in SBF solutions for various periods were conducted to investigate bone-like apatite formation on the surface and inside the structure of WPC samples to understand the mechanism of the phase transformation on WPC. The physical and mechanical properties of these samples before and after *in vitro* testing were investigated and reported. The density, porosity and compressive strength of the WPC samples were measured according to ASTM standards. Bone-like apatite precipitation was investigated using scanning electron microscopy (SEM), energy dispersive spectroscopy (EDS) and X-ray diffraction (XRD) techniques.

2. Materials and methods

2.1 Material and sample preparation

The WPC used in this study is composed mainly of a high amount of CaO (78.77%) and smaller quantities of SiO_2 (14.68%) and Al_2O_3 (1.93%). It is similar to Portland cement according to the ASTM C150 standard [25]. WPC pastes were prepared with distilled water at a cement to liquid ratio of 2:1 by mass. The WPC pastes were cast into 25×25×25 mm^3 acrylic cubic moulds for the compressive strength tests and into 10 mm diameter and 2 mm high acrylic cylindrical disc moulds for the *in vitro* bioactivity tests. The freshly mixed samples were compacted using a vibrating machine for 15 seconds to remove entrapped air, wrapped with a plastic sheet and then cured in a temperature-controlled chamber at 23 °C for 24 hours. After curing, samples were removed from their moulds and then cured in water for 3, 7, 14, 21 and 28 days at 23 °C in a temperature-controlled chamber to study the strength development of WPC during the hydration reaction. The hydration of the samples was halted by soaking them in acetone for 24 hours, drying them at 40 °C for 24 hours and storing them in a desiccator. The sample after curing in water for 28 days and stopping of hydration reaction is denoted as as-cured sample.

2.2 Setting time, density, porosity and compressive strength of WPC

Setting times for WPC pastes were determined using a Vicat needle as specified by ASTM C191 [26]. Density and porosity (permeable voids) of the WPC samples were measured using cube-shaped samples according to ASTM C642-97 [27]. To determine the density and the porosity of the samples after curing for 3, 7, 14, 21 or 28 days in water, the samples were boiled in water for 5 hours and allowed to cool for 24 hours. The masses of the cured and boiled samples suspended in water were then recorded. This was the apparent mass, A. The surfaces of the cured and boiled samples were dried with a towel and then their masses were measured. This mass was the saturated surface-dry mass, B. After that, the cured samples were dried in an incubator at 100 °C for 48 hours and allowed to cool in a desiccator to room temperature. Their masses were then determined and are denoted by the dried mass, C. The density and volume of permeable voids (porosity) were determined using the following equations:

$$Density\ (g/cm^3) = \frac{B}{(B-A)} \times \rho W : \rho W = 1\ (g/cm^3) \quad (1)$$

$$Volume\ of\ permeable\ void\ (\%) = \frac{(B-C)}{(B-A)} \times 100 \quad (2)$$

Compressive strength tests were conducted on cube-shaped samples in accordance with ASTM C109 [28] using a hydraulic testing machine with a maximum load of 400 kN. The compressive strength of the cured samples was tested at a loading rate of 2 kN/s. The density, permeable voids and compressive strength of the samples were measured after 3, 7, 14, 21 and 28 days of curing. The reported results are the averages of five measurements.

2.3 In vitro test and sample characterizations

The as-cured cube- and disc-shaped samples were submerged in SBF solutions for various periods to study the effect of an *in vitro* environment on their compressive strengths and bone-like apatite precipitation. The immersion periods were varied from 3-28 days. The temperature was controlled at 37 °C, human body temperature, for the entire immersion period. The SBF solution had an ionic concentration similar to that of human blood plasma and was prepared according to the procedure described by Kokubo et al. [29]. In order to clearly investigate the effects of *in vitro* immersion on the strength of the WPC samples, two batches of as-cured cube-shaped samples (samples after curing in water for 28 days) were then separately immerged in SBF solution and in water for the same periods at 37 °C. Their compressive strengths were measured on dried samples after immersion for 3-28 days. The averages of five samples were reported to assure uniformity of the results according to ASTM C109. In order to observe and verify bone-like apatite precipitation, surface and cross-sectional morphologies of the as-cured disc samples were examined by SEM (Zeiss LEO Model 1430) before immersion in the SBF solution. The elemental composition on the surfaces and in cross-sections of the as-cured disc-shaped samples was determined using EDS. Additionally, the crystalline phases on the surfaces of the cured disc-shaped samples were identified using XRD (Bruker D8). The XRD analysis was done with Cu Kα radiation operating at 40 kV and 40 mA at a scanning rate of 2.4° 2θ/min in 0.02° 2θ increments. After immersion in the SBF solution for various periods, the samples were removed from the

solution, carefully washed with distilled water and air-dried in the room environment. The crystalline phase, morphology and elemental composition of the surfaces and cross-sections of the WPC disc samples were investigated using XRD and SEM/EDS.

3. Results and discussion

3.1 Setting time, density and porosity of WPC

The results of the initial and final setting times of the WPC pastes were 216 and 270 min, respectively. These setting times are in the range of those described in ASTM C191. These results imply that a WPC was undergone normal hydration. After curing for 3, 7, 14, 21 and 28 days, the density and porosity of the samples were measured following the ASTM standard. The results are shown in Figure 1. The density of WPC increased with increased curing time, while the porosity of WPC decreased. The density and porosity ranged from 1.72 to 1.82 g/cm^3 and from 45.77 to 41.83%, respectively. The changes in density and porosity were due to the hydration reaction of WPC while curing in water. The average reported density of hydrated cortical bone is 1.85 g/cm^3 [30]. The WPC degree of hydration has a direct effect on its porosity and strength [31]. Higher porosities in bone substitute materials imply a larger surface area, which may result in a higher degree of bone formation after implantation in a physiological environment. An ideal porous bone substitute should provide sufficient porosity for bone ingrowth. Although increased porosity of bone substitute materials promotes new bone growth, another consequence of increased porosity is reduced mechanical strength. Therefore, a balance between mechanical properties and biological performance is required to suit the intended application [32]. Sakamoto and Matsumoto demonstrated that a 30 to 40% porosity of ceramic bone substitute materials is useful as a spinous process spacer for laminoplasty, while a 40 to 60% porosity is required for the calvaria plate since it requires proper bone formation [33].

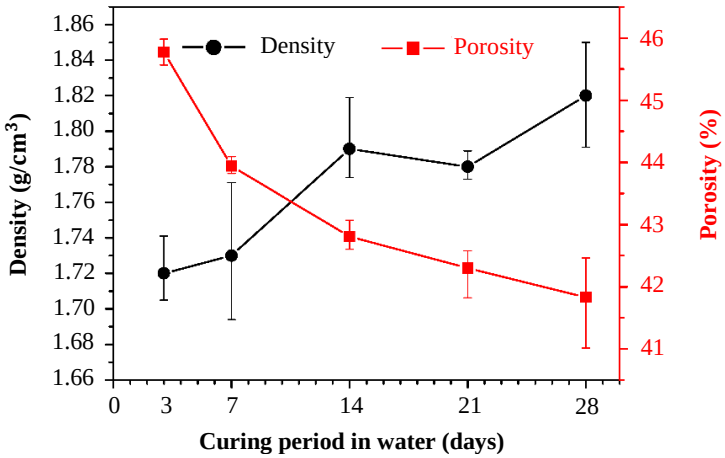

Figure 1 Average density and porosity of WPC during curing in water for various periods of time.

3.2 Compressive strength of WPC after curing and after immersion in SBF solution

The compressive strength results of WPC after curing in water and after immersion in an SBF solution are shown in Figure 2. The compressive strengths of cube-shaped samples were reported as the average measurements of five separate samples for each curing period. From the results, the compressive strength of each sample exposed to the same conditions was not manifestly different, in accordance with ASTM C109. WPC is primarily composed of calcium silicates (tricalcium silicate and dicalcium silicate). When it reacts with distilled water, it undergoes a hydration process forming ettringite, calcium hydroxide ($Ca(OH)_2$) and calcium silicate hydrate (C-S-H), which contributes to the development of strength in high alkalinities [34]. Figure 2 (a) shows the average compressive strength of the WPC samples after various curing periods of up to 28 days. The compressive strength rapidly increased early in the experiment and then only slightly increased after 21 to 28 days. This result indicated that the hydration reaction of WPC was almost completed after 28 days of curing periods. An inverse relationship was observed between the compressive strength and porosity of the WPC samples. The compressive strength of the WPC samples increased as the porosity decreased to form a denser hydration product. After 28 days of curing in water, WPC samples achieved average compressive strengths of 51.88 MPa. Since this material is planned for use as a bone substitute, WPC samples with this strength have the potential for bone repair. The compressive strength of cancellous bone ranges between 2 and 45 MPa [2, 30, 35].

To study the effect of immersion in an SBF solution on compressive strength of WPC, the as-cured samples were separately immersed in SBF solution and in water for various periods (3, 7, 14 and 28 days) at 37 °C. The compressive strength tests were conducted on dried samples after immersion in SBF solution and in water. The results are shown in Figure 2 (b). All cured WPC samples immersed in an SBF solution and water showed higher compressive strengths than those of the WPC samples after curing in water (Figure 2 (a)). After four weeks of immersion, the compressive strengths of the WPC samples gradually increased to 59.02 and 58.07 MPa for the SBF solution and water, respectively. The improvement in compressive strength was about 13 percent when compared to the strength of as-cured WPC sample. The increases were due to the continued hydration of the samples. The average compressive strength between all as-cured WPC samples immersed in an SBF solution and in water showed not significantly difference due to there is some deviation of the results. However, the average compressive strengths of the as-cured WPC samples immersed in the SBF solution were slightly higher than those of the samples immersed in water for each period, as shown in Figure 2 (b). The difference of the WPC strength after immersion in SBF and in water seemed to increase with increasing the immersion period. The result may due to the apatite formation on the WPC structure. This hypothesis was clarified at subtopic 3.4 cross-section characterization of WPC before and after immersion in SBF solution. The increasing strength of WPC after immersion in the SBF solution is a good indicator of its potential as a bone substitute material in a physiological environment. This is in contrast to HAp, whose strength decreases with increasing immersion periods in a physiological environment.

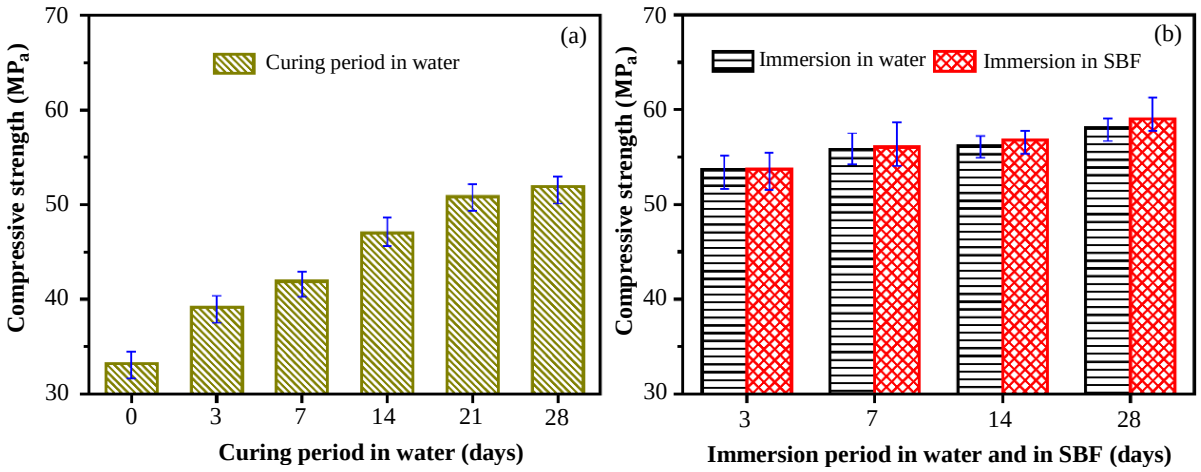

Figure 2 The average compressive strength of (a) WPC after curing in water and (b) as-cured WPC samples after immersion in water and in an SBF solution for various periods of time.

3.3 Surface characterization of WPC before and after immersion in SBF solution

The surface morphology and elemental composition of as-cured WPC sample (sample after curing in water for 28 days) were observed using SEM/EDS (Figure 3). Dense and rough structures with micropores were observed on the surface, as seen in Figure 3 (a). The results of EDS analysis of a WPC surface are shown in Figure 3 (b). The main spectrum peaks of calcium (Ca) and silicon (Si), as well as oxygen (O), corresponded to the primary elements of the WPC sample. Figure 4 shows the XRD patterns for 2θ between 20-50° and 30-40° for the as-cured WPC surface and its surfaces after immersion in SBF for various periods. The XRD pattern for the as-cured WPC surface is shown in Figure 4 (a). The major crystalline phases detected were calcite (C, peaks at 29.4°, 36.0°, 39.4°, 43.1°, 47.5° and 48.5°), portlandite (P, peaks at 28.7° and 34.1°) and ettringite (E, peak at 22.9°). The calcite peak (2θ = 29.4°) had the highest intensity in the WPC samples because of the reactions between the high CaO content in the WPC with CO_2 in the mixing water or air.

To clearly understand the mechanism of the phase transformation on WPC during immersion in an SBF solution, the as-cured WPC samples were immersed in an SBF solution for various periods ranging from 1-28 days. Figures 4 (b-f) shows the XRD patterns obtained from the as-cured WPC surfaces after immersion in the SBF solution. The phase composition of the WPC surfaces was changed. The peak intensity of the portlandite phase (28.7° and 34.1°) vanished after 1 day, which suggested that this phase dissolved during the earliest stage of immersion. After 1 day of immersion, $Ca(OH)_2$ in the form of portlandite started to dissolve into the SBF solution. It has been reported that a high concentration of calcium hydroxide is released from the WPC matrix into an SBF solution [21, 36]. The released OH^- was partially buffered by the SBF solution. This resulted in an increased pH in the SBF solution, as depicted in Figure 5. With increased immersion time, the pH of the SBF solution gradually increased, then was relatively constant at 10.5 after 14 days. The peak intensity of the ettringite phase disappeared after 7 days, and those of the calcite phases decreased with increasing immersion time. These disappearances resulted from ettringite and calcite dissolving concurrently at higher pH values. Dissolution rates have been described in the literature for various minerals, including calcium silicate hydrate at around 10^{-10} to 10^{-13} mol m^{-2} s^{-1} at pH 9.5-12 [37-39]. The dissolution of portlandite, ettringite and calcium silicate hydrate occurs according to the following chemical equations:

$$Ca(OH)_2 \rightarrow Ca^{2+} + 2OH^- \quad (3)$$

$$Ca_6Al_2(SO_4)_3(OH)_{12}\cdot 26H_2O \rightarrow 6Ca^{2+} + 2Al^{3+} + 3SO_4^{2-} + 12OH^- + 26H_2O \quad (4)$$

$$xCaO\cdot SiO_2\cdot xH_2O + H_2O \rightarrow xCa^{2+} + H_3SiO^{4-} + (2x-1)OH^- \quad (5)$$

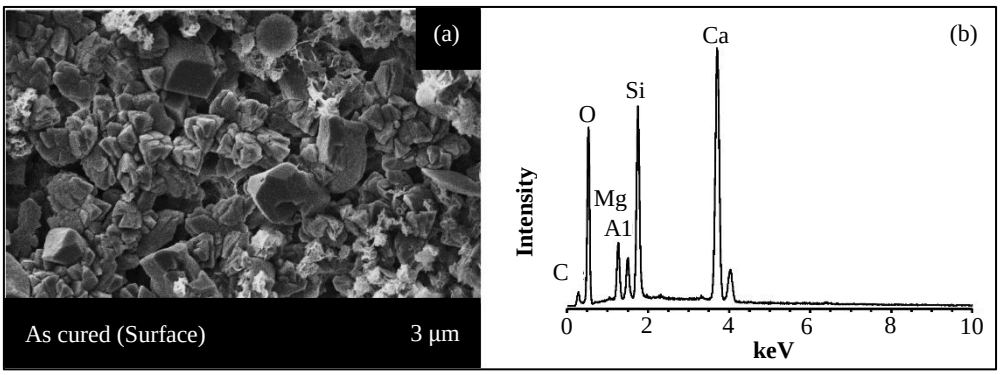

Figure 3 (a) SEM Micrographs of surface morphology of as-cured WPC sample (b) EDS Spectrum of as-cured WPC sample surface.

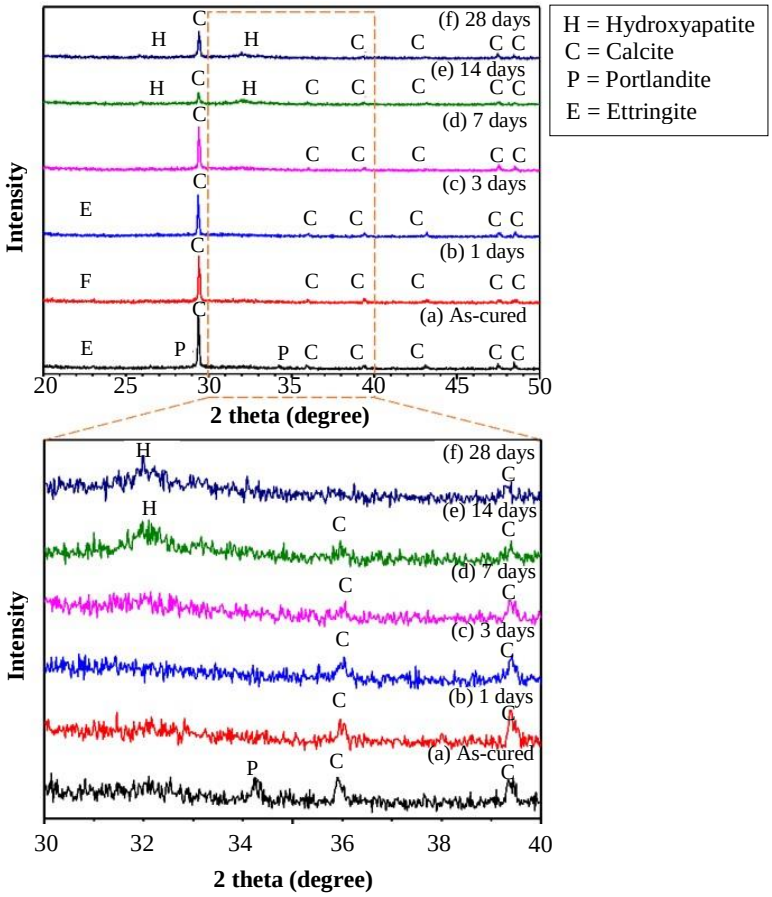

Figure 4 XRD Patterns of (a) the as-cured WPC sample and (b-f) the as-cured WPC samples after immersion in an SBF solution for various periods

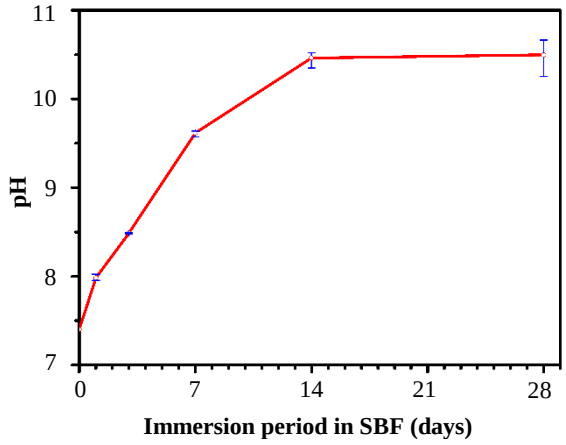

Figure 5 pH of SBF Solution during immersion of as-cured WPC samples for various periods of time.

An increased peak intensity at the 2θ position of a poorly crystalline HAp phase (H) was clearly observed at about a 2θ of 25.8° and 31-33° after 14 days of immersion, as shown in Figures 4 (e and f). This would suggest a bone-like apatite precipitation on the WPC sample surfaces. The supersaturation of ions in the SBF solution was due to the dissolution of the Ca^{2+} and OH^- of WPC. The Ca^{2+} and OH^- reacted with and in the SBF solution, resulting in the precipitation of bone-like apatite on the WPC surfaces. The precipitation of bone-like apatite occurs by the chemical equation:

$$5Ca^{2+}+3PO_4^{3-}+OH^- \rightarrow Ca_5(PO_4)_3(OH) \quad (6)$$

The driving force for this reaction and the bone-like apatite precipitation rate in a supersaturated SBF solution have been reported in the literature [40]. A supersaturated SBF solution at a high pH has a high thermodynamic driving force for the nucleation and precipitation of bone-like apatite. Additionally, recent research has reported that the degradation of calcium silicate hydrate to the Si-OH functional group in WPC during immersion in an SBF solution could act as a nucleation site for the precipitation of bone-like apatite [21-23, 29, 41, 42]. Therefore, the combination of the supersaturated ionic concentrations in the SBF solution, the increase in pH of the SBF solution and the degradation of calcium silicate hydrate to the Si-OH functional group in the WPC samples resulted in the formation of bone-like apatite. The high pH value of SBF solution during the immersion of as-cured WPC sample may cause toxicity in human cells. The extensive study of the cytotoxic of WPC is also needed in order to use as implant materials. The peak

intensity of the HAp was not observed on the samples immerged in water at all periods of immersion. Figure 6 shows SEM micrographs of the as-cured WPC surface and for those after immersion in an SBF solution. The surface texture of the as-cured WPC sample (Figure 6 (a)) changed from a rough and compact appearance with surface pores to one with tiny spherical particles after one day of immersion (Figure 6 (b)). High surface porosity with tiny spherical particles was observed after immersion in an SBF solution for three and seven days (Figures 6 (c and d)). After 14 and 28 days of immersion (Figures 6 (e and f)), the surfaces of the WPC samples were covered with a homogeneous porous network structure. This structure consisted of plate-like crystals, which characterize a bone-like apatite structure [43, 44]. The surface texture of the as-cured WPC samples was not changed during immersion in water for various periods.

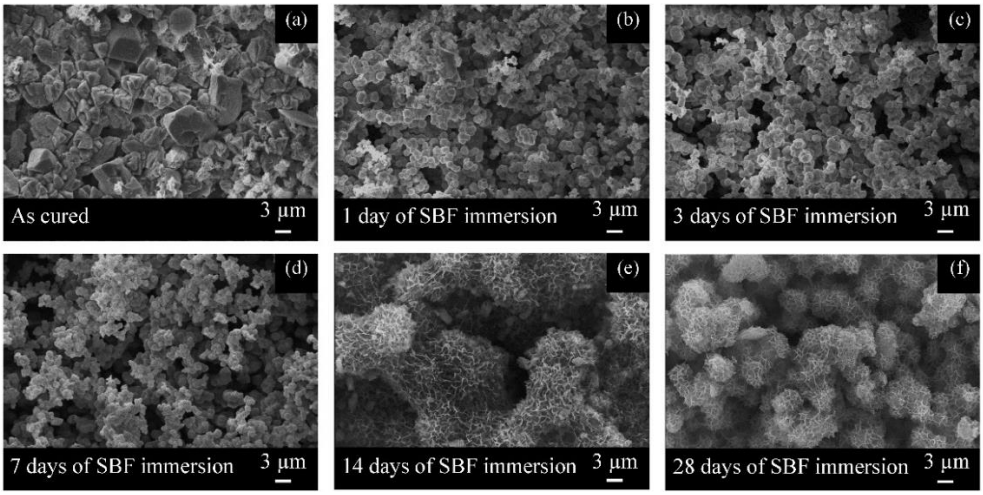

Figure 6 SEM Micrographs of surfaces of (a) the as-cured WPC samples and the as-cured WPC samples after immersion in an SBF solution for (b) 1 day (c) 3 days (d) 7 days (e) 14 days and (f) 28 days.

The results of the EDS analysis of the as-cured WPC surface and for those after immersion for 14 and 28 days in an SBF solution are shown in Figures 7 (a-c). Primarily, calcium (Ca), silicon (Si), magnesium (Mg) and aluminium (Al) were observed in the EDS spectrum of a WPC surface before immersion in the SBF solution (Figure 7 (a)). The EDS spectra of WPC after immersion periods of 14 and 28 days in an SBF solution are displayed in Figures 7 (b and c). These spectra show the presence of phosphorus (P) in addition to Ca, Si, Mg and Al at the WPC surfaces. In the EDS profiles, the intensity of the peak of P increased and those of Ca changed with increasing immersion periods in comparison with those before immersion in the SBF solution. The evidence from XRD, EDS and morphology observations confirms the precipitation of a bone-like apatite structure on WPC surfaces *in vitro* during SBF solution immersion. The peak intensity of other elements (Si, Mg and Al) decreased after SBF immersion for 14 and 28 days due to the bone-like apatite precipitation on the WPC surface.

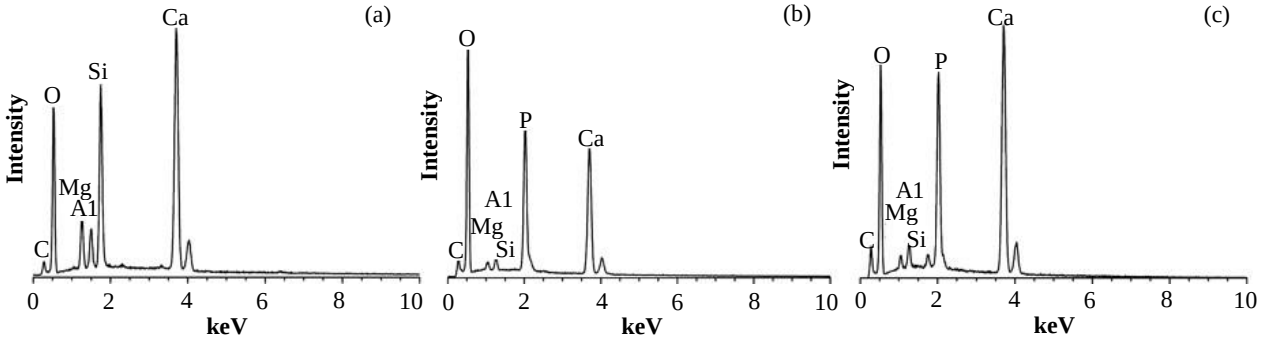

Figure 7 EDS Spectrum of surfaces of (a) the as-cured WPC samples and the as-cured WPC samples after immersion in an SBF solution for (b) 14 days and (c) 28 days.

3.4 Cross-section characterization of WPC before and after immersion in SBF solution

Cross-sectional microstructure observations and line scanning were also performed using SEM/EDS from the surface to the interior of the as-cured WPC samples and for those immersed in an SBF solution for 14 and 28 days. Line scanning measurements were made at every 0.5 µm. The spectra of silicon (Si), calcium (Ca) and phosphorus (P) were investigated. The results are shown in Figure 8. Figure 8 (a) shows the cross-sectional microstructure near the surface of the as-cured WPC sample. It was found that a dense and porous structure was formed. Only high-intensity spectra for Ca and Si were detected before immersion in the SBF solution. These are the elements of hydrated WPC presented in Eqn. (3-5). Phosphorus was not detected along the scan line. A strong spectrum for P was detected at the surface of the WPC sample after immersion in SBF solution for 14 and 28 days, as shown in Figures 8 (b and c). Phosphorus was detected up to 20 or 30 µm into the interior of the material after immersion in the SBF solution for 14 and 28 days, respectively. From these results, it can be concluded that bone-like apatite precipitated primarily on the surface of WPC to about 30 µm deep after immersion in an SBF solution for 28 days. Moreover, the small phosphorus spectrum was detected inside the WPC samples (Figures 8 (b and c)). This result indicated that the bone-like apatite also precipitated inside the structure of WPC. From the SEM micrographs in Figure 8 (b and c), there was a clear formation of bone-like apatite on the surfaces of WPC samples. Additionally,

the pore volume inside the samples tended to decrease with increasing immersion. These results also indicated that bone-like apatite was also precipitated inside the internal structure of WPC samples. This internal formation of bone-like apatite would affect the strength of WPC due to changes in its porosity and density of the samples. As shown in Figure 2 (b), the average compressive strengths of cured WPC samples after immersion in an SBF solution were slightly higher than those of samples immersed in water for longer than 7 days. These results support the potential for WPC to study as a coating material on metallic implants and bone repair applications. Therefore, a future study is needed to examine clearly the effects of immersion in an SBF solution on the strength of WPC to determine whether bone-like apatite formation on WPC improves its compressive strength and the other properties (e.g., tensile strength, stress-strain behavior). The extensive study of the cytotoxic of WPC is also needed in order to use as implant material.

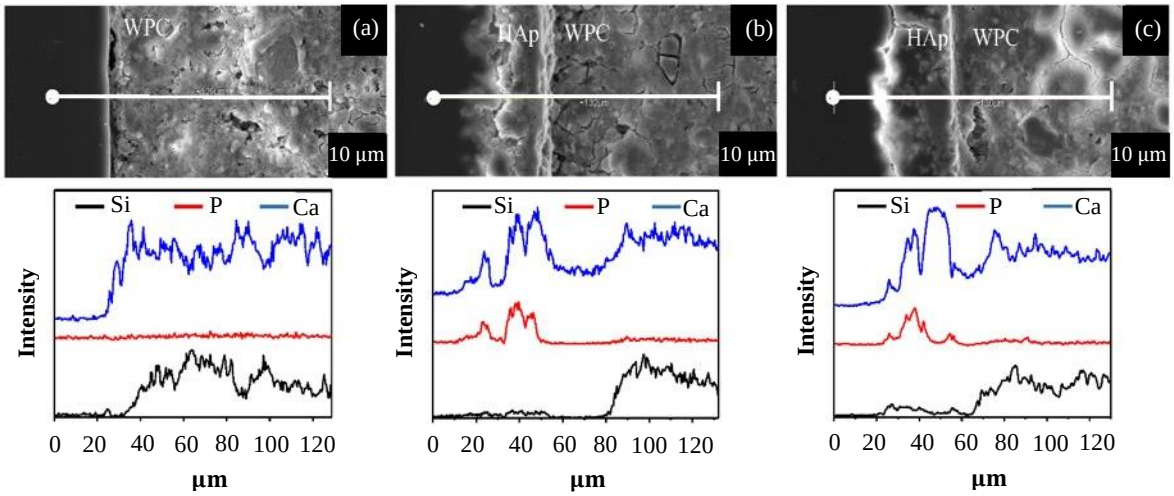

Figure 8 SEM Micrographs and scan line EDS spectra of a cross-sectional structure of (a) the as-cured WPC samples and the as-cured WPC samples after immersion in an SBF solution for (b) 14 days and (c) 28 days.

4. Conclusions

The effects of in vitro immersion in an SBF environment on the physical characteristics and compressive strength of WPC were examined. The conclusions of the current study are as follows:

(1) The compressive strength of WPC sample was 51.88 MPa after curing in water for 28 days and its porosity was 41.83%. After 28 days of immersion in an SBF solution, the compressive strengths of WPC samples showed noticeable improvements, increasing to 59.02 MPa. The increasing WPC strength during immersion in an SBF is a good indicator of its potential application as a bone substitute material in a physiological environment.

(2) WPC shows good bioactivity. During immersion in the SBF solution, WPC compounds were dissolved in the SBF solution and were precipitated as bone-like apatite on the surface of WPC. This process was clearly observed after seven days of immersion.

(3) Bone-like apatite was formed mainly on the surface of WPC with thicknesses of 20 and 30 µm after immersion in an SBF solution for 14 and 28 days, respectively. Additionally, bone-like apatite was also precipitated inside the internal structure of WPC.

5. Acknowledgements

This research was supported by the Thailand Research Fund and the Office of the Higher Education Commission [Grant No. MRG6180026], the Capacity Building Program for New Researcher 2018 from National Research Council of Thailand (NRCT) and the Faculty of Engineering, Khon Kaen University, Thailand. The second author would like to acknowledge the support of Thailand Research Fund (TRF) under the TRF Distinguished Research Professor Grant No. DPG6180002. The last author would like to acknowledge support of the Supply Chain and Logistics System Research Unit, Faculty of Engineering, Khon Kaen University, Thailand.

6. References

[1] Prasadh S, Wong R. Unraveling the mechanical strength of biomaterials used as a bone scaffold in oral and maxillofacial defects. Oral Sci Int. 2018;15(2):48-55.
[2] Hannink G, Arts JJ. Bioresorbability, porosity and mechanical strength of bone substitutes: what is optimal for bone regeneration?. Injury. 2011;42(2):S22-5.
[3] Kokubo T. Bioactive glass ceramics: properties and applications. Biomaterials. 1991;12(2):155-63.
[4] Mukherjee S, Kundu B, Sen S, Chanda A. Improved properties of hydroxyapatite-carbon nanotube biocomposite: mechanical, in vitro bioactivity and biological studies. Ceram Int. 2014;40:5635-43.
[5] Tolga Demirtaş T, Kaynak G, Gumuşderelioglu M. Bone-like hydroxyapatite precipitated from 10×SBF-like solution by microwave irradiation. Mater Sci Eng C Mater Biol Appl. 2015;49:713-9.
[6] Lee TC, Koshy P, Abdullah HZ, Idris MI. Precipitation of bone-like apatite on anodised titanium in simulated body fluid under UV irradiation. Surf Coating Technol. 2016;301:20-8.
[7] Leena M, Rana D, Webster TJ, Ramalingam M. Accelerated synthesis of biomimetic nano hydroxyapatite using simulated body fluid. Mater Chem Phys. 2016;180:166-72.
[8] Wang Y, Yang X, Gu Z, Qin H, Li L, Liu J, et al. In vitro study on the degradation of lithium-doped hydroxyapatite for bone tissue engineering scaffold. Mater Sci Eng C. 2016;66:185-92.
[9] Ke D, Vu AA, Bandyopadhyay A, Bose S. Compositionally graded doped hydroxyapatite coating on titanium using laser and plasma spray deposition for bone implants. Acta Biomater. 2019;84:414-23.

[10] Tian YS, Qian XL, Chen MQ. Effect of saturated steam treatment on the crystallinity of plasma-sprayed hydroxyapatite coatings. Surf Coating Technol. 2015;266:38-41.
[11] Fernandez J, Gaona M, Guilemany JM. Effect of heat treatments on HVOF hydroxyapatite coatings. J Therm Spray Technol. 2007;16(2):220-8.
[12] Singh G, Singh S, Prakash S. Surface characterization of plasma sprayed pure and reinforced hydroxyapatite coating on Ti6Al4V alloy. Surf Coating Technol. 2011;205(20):4814-20.
[13] Rattan V, Sidhu TS, Mittal M. Study and characterization of mechanical and electrochemical corrosion properties of plasma sprayed hydroxyapatite coatings on AISI 304L stainless steel. J Biomimet Biomater Biomed Eng. 2018;35:20-34.
[14] Latka L, Pawlowski L, Chicot D, Pierlot C, Petit F. Mechanical properties of suspension plasma sprayed hydroxyapatite coatings submitted to simulated body fluid. Surf Coating Technol. 2010;205(4):954-60.
[15] Zhang Y, Wu Z, Shu Y, Wang F, Cao W, Li W. A novel bioactive vaterite-containing tricalcium silicate bone cement by self hydration synthesis and its biological properties. Mater Sci Eng C Mater Biol Appl. 2017;79:23-9.
[16] Feng P, Wei P, Li P, Gao C, Shuai C, Peng S. Calcium silicate ceramic scaffolds toughened with hydroxyapatite whiskers for bone tissue engineering. Mater Char. 2014;97:47-56.
[17] Prati C, Gandolfi MG. Calcium silicate bioactive cements: biological perspectives and clinical applications. Dent Mater. 2015;31(4):351-70.
[18] Coleman NJ, Li Q. The impact of iodoform on the hydration, bioactivity and antimicrobial properties of white Portland cement. MATEC Web Conf. 2017;109:04002.
[19] Pu Y, Huang Y, Qi S, Chen C, Seo HJ. In situ hydroxyapatite nanofiber growth on calcium borate silicate ceramics in SBF and its structural characteristics. Mater Sci Eng C Mater Biol Appl. 2015;55:126-30.
[20] Shirazi FS, Mehrali M, Oshkour AA, Metselaar HS, Kadri NA, Abu Osman NA. Mechanical and physical properties of calcium silicate/alumina composite for biomedical engineering applications. J Mech Behav Biomed Mater. 2014;30:168-75.
[21] Coleman NJ, Awosanya K, Nicholson JW. Aspects of the in vitro bioactivity of hydraulic calcium (alumino) silicate cement. J Biomed Mater Res A. 2009;90(1):166-74.
[22] Coleman NJ, Nicholson JW, Awosanya K. A preliminary investigation of the in vitro bioactivity of white Portland cement. Cement Concr Res. 2007;37(11):1518-23.
[23] Torkittikul P, Chaipanich A. Investigation of the mechanical and in vitro biological properties of ordinary and white Portland cements. Sci Asia. 2009;35(4):358-64.
[24] Abdullah D, Ford TR, Papaioannou S, Nicholson J, McDonald F. An evaluation of accelerated Portland cement as a restorative material. Biomaterials. 2002;23(19):4001-10.
[25] ASTM. ASTM C150-07, Standard specification for Portland cement. West Conshohocken: ASTM; 2007.
[26] ASTM. ASTM C 191-99, Standard test method for time of setting of hydraulic cement by Vicat Needle. West Conshohocken: ASTM; 1999.
[27] ASTM. ASTM C 642-13, Standard test method for density, absorption, and voids in hardened concrete. West Conshohocken: ASTM; 2013.
[28] ASTM. ASTM C109. /C109M-16a, Standard Test Method for Compressive Strength of Hydraulic Cement Mortars (Using 2-in. or [50-mm] Cube Specimens). West Conshohocken: ASTM; 2016.
[29] Kokubo T, Takadama H. How useful is SBF in predicting in vivo bone bioactivity?. Biomaterials. 2006;27(15):2907-15.
[30] Keaveny TM, Morgan EF, Yeh OC. Chapter 8 bone mechanics. In: Kutz M, editor. Standard handbook of biomedical engineering and design. New York: McGraw-Hill; 2004. p. 8.1-8.23.
[31] Jankovic K, Nikolic D, Bojovic D, Loncar L, Romakov Z. The estimation of compressive strength of normal and recycled aggregate concrete. Facta Univ Architect Civ Eng. 2011;9(3):419-31.
[32] de Vasconcellos LM, Nascimento RD, Cairo C, de Oliveira Leite D, de Souza Santos EL, Campos GE, et al. Porous titanium associated with CaP coating: in vivo and in vitro osteogenic performance. Mater Res. 2018;21(2):1-5.
[33] Sakamoto M, Matsumoto T. Development and evaluation of superporous ceramics bone tissue scaffold materials with triple pore structure a) hydroxyapatite, b) beta-tricalcium phosphate. In: Tal H, editor. Bone Regeneration. London: Intech Open; 2012. p. 301-20.
[34] Veiga KK, Gastaldini ALG. Sulfate attack on a white Portland cement with activated slag. Construct Build Mater. 2012;34: 494-503.
[35] Suchanek W, Yoshimura M. Processing and properties of hydroxyapatite-based biomaterials for use as hard tissue replacement implants. J Mater Res. 1998;13(01):94-117.
[36] Li Q, Coleman NJ. Hydration kinetics, ion-release and antimicrobial properties of white Portland cement blended with zirconium oxide nanoparticles. Dent Mater J. 2014;33(6):805-10.
[37] Soler JM. Thermodynamic description of the solubility of C-S-H gels in hydrated Portland cement. Literature review. Posiva Work Rep. 2007;43(29):1-38.
[38] Myneni SCB, Traina SJ, Logan TJ. Ettringite solubility and geochemistry of the $Ca(OH)_2$-$Al_2(SO_4)_3$-H_2O system at 1 atm pressure and 298 K. Chem Geol. 1998;148(1-2):1-19.
[39] Baur I, Keller P, Mavrocordatos D, Wehrli B, Johnson CA. Dissolution-precipitation behaviour of ettringite, monosulfate, and calcium silicate hydrate. Cement Concr Res. 2004;34(2):341-8.
[40] Lu X, Leng Y. Theoretical analysis of calcium phosphate precipitation in simulated body fluid. Biomaterials. 2005;26(10): 1097-108.
[41] Lin K, Zhai D, Zhang N, Kawazoe N, Chen G, Chang J. Fabrication and characterization of bioactive calcium silicate microspheres for drug delivery. Ceram Int. 2014;40(2):3287-93.
[42] Niu LN, Jiao K, Wang TD, Zhang W, Camilleri J, Bergeron BE, et al. A review of the bioactivity of hydraulic calcium silicate cements. J Dent. 2014;42(5):517-33.
[43] Takeshi Y. Biomimetic porous bone-like apatite coatings on metals, organic polymers and microparticles. In: Al-Naib UB, editor. Recent Advances in Porous Ceramics. London: Intech Open; 2017. p. 11-30.
[44] Drouet C. Apatite formation: why it may not work as planned, and how to conclusively identify apatite compounds. Biomed Res Int. 2013;2013(4):490946.